https://doi.org/10.5194/hess-2020-441
Preprint. Discussion started: 14 September 2020

Hydrology and Earth System Sciences
Discussions

Impacts of land use/cover change and reforestation on summer rainfall for the Yangtze River Basin

Wei Li[1,2], Lu Li[3], Jie Chen[1,2], Qian Lin[1,2], Hua Chen[1,2]

[1]State Key Laboratory of Water Resources and Hydropower Engineering Science, Wuhan University, Wuhan, 430072, China
[2]Hubei Key Laboratory of Water System Science for Sponge City Construction, Wuhan University, Wuhan, 430072, China
[3]NORCE Norwegian Research Centre, Bjerknes Centre for Climate Research, Bergen, 5238, Norway

Corresponding to: Jie Chen (jiechen@whu.edu.cn)

Abstract. Land use and cover has been significantly changed all around the world during the last decade. In particular, the Returning Farmland to Forest Program (RFFP) have resulted in significant changes in regional land use and cover, especially in China. The land use and cover change (LUCC) may lead to the change in regional climate. In this study, we take the Yangtze river basin as a case study and analyze the impacts of LUCC and reforestation on summer rainfall amount and extremes based on the Weather Research and Forecasting model. Firstly, two observed land use and cover scenarios (1990 and 2010) were chosen to investigate the impacts of LUCC on the summer rainfall during the last decade. Secondly, two hypothetical reforestation scenarios (i.e., scenarios of 20% and 50% cropland changed to be forest) were taken based on the control year of 2010 to test the sensitivity of summer rainfall (amount and extremes) to reforestation. The results showed that LUCC between 1990 and 2010 decreased average summer rainfall, while increased extreme summer daily rainfall in the Yangtze River basin. The extreme summer daily rainfall increased up to 50 mm, which was mainly observed in the midstream and downstream. Reforestation could increase summer rainfall amount and extremes, and the effects were more pronounced at the local scale where suffered reforestation than at the whole basin. Moreover, the effects of reforestation were influenced by the reforestation proportion. In this study, the average summer rainfall increased more for the scenario of 20% croplands changed to forests than that for the scenario of 50%, while the high-intensity short-duration rainfall increased more for the scenario of 50% croplands changed to forests than that for the scenario of 20%. Although a comprehensive assessment of the impacts of LUCC on summer rainfall amount and extremes was conducted, further studies are needed to better investigate the uncertainty.

1 Introduction

Human activities intensified land use and land cover change (LUCC) all around the world. With the human population increasing, more than one-third of global natural land uses were altered by human activities during the past three centuries (Hurtt et al., , 2006, 2011). The land surface was the lower boundary of atmospheric motion. Thus, LUCC could influence climate through various geophysical processes, such as the water and heat flux between land surface and atmosphere, surface wind speed, and boundary layer turbulence. LUCC could affect regional climate significantly, which had become a broad

https://doi.org/10.5194/hess-2020-441
Preprint. Discussion started: 14 September 2020


Hydrology and Earth System Sciences
Discussions

consensus as many studies proved this. For instance, Pitman et al. (2012) found that many of the temperature indices showed locally strong and statistically significant responses to LUCC, such as that commonly 30-50% of the continental surfaces of the tropics and Northern and Southern Hemispheres were affected statistically significantly by LUCC. Wen et al. (2013) also found that the land-use change in China could contribute to the warmest day temperature increases. Yira et al. (2016) also showed that due to the decrease of savannah and increase of cropland and urban area in the Dano catchment over Burkina Faso, apparent evapotranspiration decrease (-5%) was observed following land-use changes in the catchment. Besides, Davin et al. (2020) explored the impacts of reforestation over Europe based on nine RCMs and found that reforestation would result in a winter warming effect which ranged from 0.2 to 1 K on average over Scandinavia depending on models.

China is experiencing significant changes in land use due to human activities, especially for the high-population-density Yangtze River basin (YRB). The Yangtze River is the longest river in Asia and the third-longest in the world with a length over 6300 km. The YRB is the largest basin in China, which supports 34% of the nation's population and contributes 41.1% of China's gross domestic products (Zhang et al., 2014). Considering agricultural activities, urbanization, and dam construction, LUCC is quite significant in this basin (Liu et al., 2003;Zhang et al., 2009;Shen et al., 2019). Moreover, China launched the Returning Farmland to Forest Program (RFFP) to expand forestland since 1999, aiming to reduce soil erosion and alleviate poverty (Robbins and Harrell, 2014;Li et al., 2020). From 1999 to 2008, forest coverage, reported as a percentage of the country's total land area increased from 16.55 % to 20.36 %, adding 41.6 million ha of forest (Trac et al., 2013). By 2013, China government had invested over 320 billion RMB in afforesting over 29 million hectares (Zinda et al., 2017). The RFFP focused on increasing forest cover through cropland conversion and afforestation and reforestation of barren hillsides. Sloping cropland was a core target of the program, which was blamed for 65% of the 2 to 4 billion tons of silts released into the Yangtze and middle and upper reaches of the Yellow River each year (Bennett et al., 2011). Because of the RFFP, there was also a trend of LUCC in the YRB that returning cropland to forest. All the LUCC in the YRB changed the regional climate during the past few decades. For example, Cui et al. (2012) found that reforestation could increase evapotranspiration and decrease water yield at the forest stand level in the upper reach of the YRB. Liu et al. (2013) displayed that reforestation in the upstream of the YRB increased annual evapotranspiration, leading to reductions in surface flow and baseflow. Besides, Hu et al. (2015) found that LUCC in eastern China caused a decrease in rainfall over the lower reaches of the YRB of approximately 3% in the summer from the 1980s to the 2000s. Zhang et al. (2017) showed that the temperature decreased by 0.2-0.4℃ in the midstream and downstream of the YRB in spring, autumn and winter, and the seasonal rainfall also decreased from the 1980s to the 2000s due to LUCC. Furthermore, Feng et al. (2018) showed that the land surface temperature over the Taihu Lake Basin, which was located in the lower reaches of the YRB, has been increasing since 1996 caused by local urbanization.

https://doi.org/10.5194/hess-2020-441
Preprint. Discussion started: 14 September 2020


Hydrology and Earth System Sciences
Discussions

The YRB plays a vital role in the ecosystem protection and economic development for the whole country. However, the YRB suffered from the flooding frequently during the past decades. Summer rainfall is the leading cause of summer flooding in the YRB which largely influences the lives of local people. Thus, it is crucial to better understand the impacts of LUCC on summer rainfall in the YRB, especially the effects of the RFFP reforestation program. Although many studies estimated the impacts of LUCC on rainfall in the YRB, it should be noted that most of the previous studies only focused on the midstream and downstream of the YRB. Moreover, the sensitivity of summer rainfall to reforestation in the YRB was rarely investigated. And few previous studies discussed the potential physical mechanisms linked to the changes in summer rainfall under reforestation. To investigate the impacts of LUCC, especially the reforestation on rainfall is of great importance for the economic and ecological development for the YRB as well as for China. There is an urgent need considering the Yangtze River Coordinated Protection Strategy proposed by the Chinese government in 2016, aiming at giving priority to ecology and green development, promoting well-coordinated environmental conservation and avoiding excessive development.

Therefore, this study took the YRB as a case study and investigated the impact of LUCC and reforestation on summer rainfall and extreme hazards. More specifically, two observed LUCC scenarios were chosen to study the impacts of observed LUCC on summer rainfall including both amount and extremes, while two hypothetical reforestation scenarios were taken to quantitively assess the impacts of reforestation on summer rainfall (amount and extremes) under different reforestation proportions. The differences of summer rainfall between the four land-use scenarios (two observed and two hypothetical ones) were applied and investigated based on the Weather Research and Forecasting (WRF) model. The major objectives of this study were to: (1) estimate the impacts of LUCC and reforestation on summer rainfall (amount and extremes) in the YRB; and (2) investigate how the proportion of reforestation effects summer rainfall (amount and extremes) in the YRB.

To better understand the impacts of LUCC and reforestation on summer rainfall, the performance of WRF-simulated rainfall was first evaluated in section 4.1. Then, the changes in summer rainfall between the 1990 scenario and 2010 scenario were analyzed to investigate the impacts of observed LUCC on summer rainfall in section 4.2. In section 4.3.1 and 4.3.2, the impacts of reforestation on summer rainfall were analyzed based on the spatial changes and area average changes, respectively. Moreover, in section 4.3.3 and 4.3.4, the impacts of reforestation on some other climate variables which were related to the rainfall were also investigated. These climate variables contained the surface skin temperature, 2m relative humidity, LHF, SHF and PBLH. The analyses of these variables were aimed at explaining the potential mechanisms of the changes in summer rainfall under reforestation. The discussions and conclusions are given at the end. Our results will contribute to a better understanding of regional climate characteristics (summer rainfall and extremes) under the impacts of LUCC and reforestation program in the YRB, and provide a knowledge base for ecological reconstruction programs in the future.

https://doi.org/10.5194/hess-2020-441
Preprint. Discussion started: 14 September 2020

Hydrology and Earth System Sciences
Discussions

2 Study area and data

2.1 Study area

This study focuses on YRB (Fig. 1), which has a total area of ~1.8×10^6 km^2 (Wang et al., 2018). The YRB is located between 24°-35°N and 90°-122°E, spanning from the eastern Tibetan Plateau to the East China Sea and crossing 19 provinces in China. The upper, middle, and lower reaches of the YRB cover 1.0×10^6 km^2, 6.8×10^5 km^2, and 1.2×10^5 km^2, respectively (Zhang et al., 2014). LUCC in the YRB was quite significant during the past few decades. The main types of LUCC including the urbanization which leads to the conversion of cropland to the urban area in the middle and lower reaches (Liu et al., 2010, 2012;Gao et al., 2012), degradation of grassland caused by overgrazing in the headwater region (Gao et al., 2009;2010), and reforestation and afforestation as a result of the implementation of the RFFP (Liu et al., 2010;Li et al., 2014). The upper reaches of the YRB belong to a high-cold climate zone, whereas the middle and lower reaches belong to subtropical and temperate climate zones (Zhang et al., 2019a). The whole YRB is sensitive and vulnerable to climate change (Fang et al., 2010). The average air temperature ranges from 9 to 18 °C, and the average annual rainfall ranges from 692 to 1611 mm (Zhang et al., 2019a). Because of relatively good water and temperature conditions, vegetation productivity is generally high in this area. However, human activities are intensifying LUCC in the YRB from the upper reaches to the lower reaches (Sun et al., 2016), which will gradually change local climate and finally influence the agriculture production.

2.2 Data

This study used WRF simulations to investigate the impacts of LUCC on summer rainfall. The WRF model with the Advanced Research WRF dynamics solver version 3.9.1 was used (Skamarock et al., 2008). The WRF model was a flexible, state-of-the-art, non-hydrostatic, mesoscale numerical weather prediction, and atmospheric simulation system (Wagner et al., 2016). The lateral boundaries of the WRF model were forced with the 0.5° ERA-Interim reanalysis (Berrisford et al., 2011). The output variables of the WRF model contained rainfall, surface skin temperature, 2m relative humidity, latent heat flux (LHF), sensible heat flux (SHF) and planetary boundary layer height (PBLH) were used in this study to analyze the changes in rainfall under LUCC and the potential physical mechanisms.

Besides, the observed rainfall and temperature from 171 stations in the YRB were used for model validation (Fig. 1), the observed data were quality controlled and provided by the China Meteorological Data Sharing Service System. In our study, the observed data from stations were interpolated to model grids by the Inverse Distance Weight (IDW) interpolation method. More details about the observed data can be found in http://data.cma.cn/data/cdcdetail/dataCode/SURF_CLI_CHN_MUL_DAY_V3.0.html. In addition, the 1990 and 2010 land use data of the YRB were derived from the Landsat thematic mapper (TM) digital images. It was interpreted based on the

https://doi.org/10.5194/hess-2020-441
Preprint. Discussion started: 14 September 2020


Hydrology and Earth System Sciences
Discussions

geometric shape, texture features, spatial distribution of the ground objects, and the spectral characteristics in the images. Moreover, the outdoor survey and random sample check were also taken to enhance the accuracy of the land use data. The resolution of the original land-use data is 1 km. The land-use categories of the original land use data were defined by Liu et al. (2002), while the land-use categories used in the WRF were the U.S. Geological Survey (USGS) land cover categories. Thus, the land use type conversions were performed based on the rules defined in Hu et al. (2015).

3 Methods

3.1 WRF Model configuration

The WRF model was set up with two nested domains in this study (Fig. 2). The resolutions of the outer and inner domain were 75 km (95 × 82 grids) and 15 km (236 × 161 grids), respectively. The model was set up with 32 vertical levels, and the top was at 50 hPa in all domains. The simulated period was 11 years from 2000 to 2010, with the first year taken as spin-up time. The initial and lateral boundary conditions were taken from 0.5° ERA-Interim reanalysis data set. The time step was 90 s in both domains.

The choices of the microphysical scheme and cumulus parameterization are important for rainfall simulations (Li et al., 2017). According to previous studies in China (Hu et al., 2015;Zhang et al., 2019b;Feng et al., 2012;Xue et al., 2017), three microphysical schemes, i.e., Purdue Lin Scheme (Lin) (Chen and Sun, 2002), WRF Single-moment 5-class Scheme (WSM5) (Hong et al., 2004) and Eta (Ferrier) Scheme (Ferrier) (Rogers et al., 2001), and two cumulus parameterizations, i.e., Kain–Fritsch Scheme (KFN) (Kain, 2004) and Grell–Devenyi Ensemble Scheme (GD) (Grell and Dévényi, 2002), were chosen to validate the WRF model. Five parameterization schemes combinations (i.e., Lin-KFN, WSM5-KFN, Ferrier-KFN, Lin-GD and WSM5-GD) were then used to simulate the rainfall and temperature in the YRB during the 2005 summer. The simulation performance of different parameterization schemes combinations was evaluated with the Taylor diagrams (Taylor, 2001) (Fig. 3). In Fig. 3, the red dots referred to positive biases, while the blue dots referred to negative biases. Moreover, the bigger the sizes of the dots were, the larger the biases were. Finally, the Lin and GD were set as microphysical scheme and cumulus parameterization, respectively.

Besides, the Yonsei University scheme was used for planetary boundary layer (Hong et al., 2006); the Dudhia scheme for shortwave radiation (Dudhia, 1988); the RRTM scheme for longwave radiation (Mlawer et al., 1997), and the Noah–MP scheme for the land surface model (Niu et al., 2011;Yang et al., 2011).

https://doi.org/10.5194/hess-2020-441
Preprint. Discussion started: 14 September 2020


Hydrology and Earth System Sciences
Discussions

3.2 The observed land-use scenarios and hypothetical reforestation scenarios

The 1990 and 2010 land-use scenarios were chosen to estimate the impacts of observed LUCC on summer rainfall amount and extremes in this study (Fig. 4a and 4b). From 1990 to 2010, the YRB suffered significant LUCC. The main LUCC in the YRB in this period was the urbanization and reforestation, as well as the constructions of dams (Liu et al., 2003;Zhang et al., 2009;Shen et al., 2019). Furthermore, to investigate the impacts of reforestation due to the RFFP, we randomly changed 20% and 50% of the cropland to be forest based on the observed land-use scenario of 2010 (Fig. 4c and 4d). These two scenarios can be considered as two extreme cases in the progress of RFFP for the future. The hypothetical reforestation scenarios (named with 20% scenario and 50% scenario) were used in the study as well as the observed land-use in 1990 and 2010 (named with 1990 scenario and 2010 scenario). As the original land-use data in the YRB has been reclassed following the USGS land cover categories, there were two main types of cropland, i.e., dry cropland and pasture (code 2), and irrigated cropland and pasture (code 3), and three main types of forest, i.e., shrubland (code 8), savanna (code 10) and deciduous broadleaf forest (code 11). When we changed croplands to forests, the proportions of each type of croplands (forests) occupied in total croplands (forests) were kept fixed.

4 Results

4.1 WRF Model validation

Figure 5 displays the spatial distributions of biases in the average summer rainfall, extreme summer daily rainfall (the 99th percentile of daily summer rainfall), and median summer daily rainfall (the 50th percentile of daily summer rainfall) simulated by WRF relative to observation. From Fig. 5a, it can be seen that the biases of WRF-simulated average summer rainfall range from -600 mm to 1000 mm. The positive biases are mainly observed in the transaction region between Sichuan Basin and Tibet plateau, with the maximum positive biases in the front zone of Tibet plateau where the altitudes shift from low to high rapidly. The negative biases are mainly observed in the southeastern YRB, which were also found in other studies (Zhang et al., 2017). Figure 5b presents the biases of extreme summer daily rainfall simulated by WRF relative to observation, varying from -50 mm to 50 mm. The positive biases are mainly observed in the upstream area where the altitudes are higher than 1200 m, while the negative biases are mainly observed in the midstream and downstream areas with the maximum negative biases located in the southeastern YRB. Figure 5c presents the biases of median summer daily rainfall, varying from -1 to 2 mm, which are negligible compared with the biases of extreme summer daily rainfall.

https://doi.org/10.5194/hess-2020-441
Preprint. Discussion started: 14 September 2020


Hydrology and Earth System Sciences
Discussions

4.2 The impacts of LUCC between 1990 and 2010 on the summer rainfall

Figure 6 shows the differences in the average summer rainfall, extreme summer daily rainfall, and median summer daily rainfall in YRB between the 1990 and 2010 scenarios. According to the results, the differences in average summer rainfall vary from -200 mm to 200 mm over the YRB (Fig. 6a). In most places of the YRB, the average summer rainfall decreases for the 2010 scenario compared with the 1990 scenario. The increases in average summer rainfall are mainly observed in the upstream and midstream. Compared with the average summer rainfall, the changes in extreme summer daily rainfall between the 1990 and 2010 scenarios show a slightly different spatial distribution (Fig. 6b). For example, the extreme summer daily rainfall increases up to 50 mm, which is mainly observed in the midstream and downstream. Besides, the changes in median summer daily rainfall between the 1990 and 2010 scenarios range from -3 mm to 2 mm. While in most parts of the YRB, the changes in median summer daily rainfall are between -1 and 1 mm (Fig. 6c).

4.3 The impacts of reforestation on the regional climate in the YRB

4.3.1 Changes in the summer rainfall

Figure 7a and 7b show the spatial changes in the average summer rainfall between the 20% scenario and 2010 scenario, and between the 50% scenario and 2010 scenario, respectively. From the results, we can see that the average summer rainfall shows a large spatial heterogeneity over the study area. For the 20% scenario, the increases of average summer rainfall (up to 200 mm) are observed in most places of the YRB, while the decreases (up to -100 mm) are mainly observed in the upstream region. For the 50% scenario, the most significant increase in average summer rainfall is observed in the upstream of the YRB, while the most significant decrease is observed in the midstream region. When comparing the changes in average summer rainfall between the 20% and 50% scenarios, areas with an increase in average summer rainfall are wider for the 20% scenario than for the 50% scenario.

Figure 7c and 7d show the changes in the extreme summer daily rainfall between the 20% scenario and 2010 scenario, and between the 50% scenario and 2010 scenario, respectively. For the 20% scenario, the extreme summer daily rainfall increases in most places of the YRB, while the decreases are mainly observed in the midstream. For the 50% scenario, the most significant increase in the extreme summer daily rainfall (up to 50 mm) is mainly observed in the upstream of the YRB, while the most significant decrease (up to -50 mm) is mainly observed in the midstream. Besides, the decrease of the extreme summer daily rainfall for the 50% scenario (up to -50 mm) is more significant than the decrease for the 20% scenario (up to -40 mm). As for the median summer daily rainfall (Fig. 7e and 7f), the changes, ranging from -1 to 2 mm, are not obvious compared with the changes in the extreme summer daily rainfall for both 20% and 50% scenarios. The median summer daily rainfall increases in most places of the YRB for the 20% scenario, while decreases in most places of the YRB for the 50% scenario.

https://doi.org/10.5194/hess-2020-441
Preprint. Discussion started: 14 September 2020


Hydrology and Earth System Sciences
Discussions

The above results also indicate that the average summer rainfall and extreme summer daily rainfall are sensitive to the reforestation (conversion from cropland to forest), while the median summer daily rainfall is not.

4.3.2 Area average changes in rainfall

In this section, changes in rainfall between the hypothetical reforestation scenarios (20% and 50% scenarios) and 2010 scenario are analyzed based on two types of area average: one is area average based on all grids of the whole YRB (ALL-YRB), and the other area average is based on only the grids where the cropland are changed to be forest (CTF-YRB).

Figure 8 presents the changes in average summer rainfall, extreme and median summer daily rainfall between the two hypothetical reforestation scenarios and the 2010 scenario in the ALL-YRB and CTF-YRB. It can be noticed that the average, extreme, and median summer daily rainfall for both hypothetical reforestation scenarios increase comparing with the 2010 scenario. Besides, the magnitude of the increases in all indices of the summer rainfall is all larger for the 20% scenarios than those for the 50% scenarios in both ALL-YRB and CTF-YRB, except extreme summer daily rainfall of the CTF-YRB, which however increases slightly more for the 50% scenario than for the 20% scenario.

Figure 9 presents the changes in maximum 1-, 3- and 5-day summer rainfall between the two hypothetical reforestation scenarios and the 2010 scenario. For the maximum 1-day rainfall, in the ALL-YRB, the increase is more from the 20% scenario than from the 50% scenario; conversely, in the CTF-YRB, the increase is much more for the 50% scenario than for the 20% scenario. For the maximum 3-day rainfall, the increases are more for the 50% scenario than for the 20% scenario for both ALL-YRB and CTF-YRB. However, for the maximum 5-day rainfall, the increases are more for the 20% scenario than for the 50% scenario for both ALL-YRB and CTF-YRB. The results indicate that the 50% scenario results in higher intensity short-duration rainfall at the local scale within the LUCC grids (where cropland are changed to be forest) than the 20% scenario. At the meantime, the 20% scenario results in more increase in the longer-duration rainfall at both local and regional scale than the 50% scenario.

To indicate more clearly the responses and sensitivities of summer rainfall to the impacts of reforestation, the probability distribution functions (PDFs) of average summer rainfall for three scenarios (i.e., 2010, 20% and 50% scenarios) are shown in Fig. 10. To be noted that, for the CTF-YRB, the grids chosen for the calculation of the PDF for the 2010 scenario are consistent with the grids used for the hypothetical reforestation scenarios. In this case, the PDF for the 2010 scenario comparing with the 20% scenario (in the Fig. 10b) is different from the PDF for the 2010 scenario comparing with the 50% scenario (in the Fig. 10c). This is because the girds, where the cropland are changed to be the forest, are different for the 20% and 50% scenarios. Thus, the CTF-YRB is further divided into the CTF-YRB (20%) and CTF-YRB (50%) in Fig. 10. Figure 10a presents the PDFs of average summer rainfall for three scenarios in the ALL-YRB. The PDFs of rainfall for three scenarios are quite similar averaged in the ALL-YRB, except for the light rainfall of 2 ~ 4 mm/day, which is more for the 2010 scenario than for the 20%

https://doi.org/10.5194/hess-2020-441
Preprint. Discussion started: 14 September 2020


Hydrology and Earth System Sciences
Discussions

scenario and 50% scenario. Figure 10b presents the PDFs of rainfall for the 2010 and 20% scenarios in the CTF-YRB (20%). The PDF of rainfall for the 20% scenario is higher than that for the 2010 scenario when rainfall is around 2 ~ 13 mm/day and 17 ~ 20 mm/day. Figure 10c presents the PDFs of rainfall for the 2010 scenario and 50% scenarios in the CTF-YRB (50%). The PDF of rainfall for the 50% scenario is slightly higher than that for the 2010 scenario when rainfall is about 9 ~ 10 mm/day. Figure 11 presents the relative changes in multi-year average monthly rainfall during the summer period between the two hypothetical reforestation scenarios and the 2010 scenario in both ALL-YRB and CTF-YRB. For rainfall in both ALL-YRB and CTF-YRB, all the relative changes for the 20% and 50% scenarios are positive. In June, the relative change in rainfall for the 50% scenario is more significant than that for the 20% scenario. However, in July and August, the relative changes for the 50% scenario are smaller than those for the 20% scenario. The results indicate that (1) the reforestations, no matter for the 20% or 50% scenarios, result in the increase in summer rainfall at a local scale in the areas where have LUCC, while the results vary in the regional scale as the increase of summer rainfall averaged from the whole YRB is smaller than that averaged from the areas where have LUCC; (2) Under the impact of the reforestation, the 20% scenario results in a more significant increase of summer rainfall than the 50% scenario.

4.3.3 Changes in the latent heat flux, sensible heat flux, and PBL height

The changes in the LHF, SHF, and PBLH are investigated after analyzing the changes in rainfall under reforestation. Figure 12a and 12b show the changes in LHF between the 20% scenario and 2010 scenario, and between the 50% scenario and 2010 scenario, respectively. The spatial distributions of LHF changes for the 20% and 50% scenarios are similar. For example, the LHF increases in most places of the southeastern YRB and decreases in most places of the upstream and midstream for both scenarios. The most significant increases of LHF (up to 20 W/m2) are also mainly observed in the southeastern YRB for both scenarios. The changes in SHF have similar spatial distribution for both 20% and 50% scenarios (Fig. 12c and Fig. 12d). The SHF decreases in most places of the YRB, while the increases of SHF are mainly observed in the north YRB. The largest SHF decreases up to -15 W/m^2 are mainly seen in the southeastern YRB. However, areas with increased SHF are more for the 50% scenario than for the 20% scenario. Figure 12e and 12f show the changes in PBLH between the 20% scenario and 2010 scenario, and between the 50% scenario and 2010 scenario, respectively. The spatial distributions of PBLH change are similar for both 20% and 50% scenarios. Nevertheless, areas with PBLH increases by more than 30 m or decreases by more than -30 m is more for the 50% scenario than for the 20% scenario.

The changes in SHF caused by reforestation can alter the thermodynamic variable PBLH. From Fig. 12, it can be seen that the changes in SHF and PBLH have similar spatial pattern. When the SHF increases, it leads to the increases of PBLH, which will increase the possibility of cloud formation and finally enhance the intensity and frequency of extreme rainfall (Shem and Shepherd, 2009).

https://doi.org/10.5194/hess-2020-441
Preprint. Discussion started: 14 September 2020


Hydrology and Earth System Sciences
Discussions

4.3.4 Changes in the summer temperature and relative humidity

The changes in the summer temperature and 2m relative humidity under reforestation are also analyzed. Figure 13a and 13b present the changes in the average summer temperature between the 20% scenario and 2010 scenario, and between the 50% scenario and 2010 scenario, respectively. The temperature here refers to surface skin temperature. For the 20% scenario, the average summer temperature decreases in most places of the YRB, while the decreases are mainly observed in the central YRB. Only a few small areas in the source region and the eastern part of the YRB, the temperature increases. For the 50% scenario, areas with decreased average summer temperature are reduced compared with that for the 20% scenario. The maximum drop in the summer temperature is -0.8 ℃ for the 20% scenario and -0.6 ℃ for the 50% scenario. Meanwhile, there are significant differences between the two scenarios in some regions. For example, in the north of the central YRB, the average summer temperature increases in the 50% scenario while decreases in the 20% scenario.

Figure 13c and 13d present the changes in 2 m relative humidity between the 20% scenario and 2010 scenario, and between the 50% scenario and 2010 scenario, respectively. From the figures, we can find that the relative humidity changes for these two hypothetical reforestation scenarios have different spatial distributions. For instance, for the 20% scenario, the relative humidity increases in most places of the YRB with the most significant increases (up to 6%) in the central YRB. When comparing Fig. 13c and Fig. 13d, it can be seen that more areas with increased relative humidity can be found in the 20% scenario than in the 50% scenario. Furthermore, the relative humidity decreases in the north of the central YRB in the 50% scenario, which is not observed in the 20% scenario.

From the changes in the surface skin temperature and 2m relative humidity under reforestation, it can be seen that the 2m relative humidity decreases where the surface skin temperature increases. When the surface skin temperature increases, more moisture is carried from the surface skin to the upper atmosphere, which will finally increase the rainfall.

5 Discussions

Comparing the results from the WRF modelling with observation data, the summer rainfall from the WRF model tends to have positive biases in the northwestern YRB, while negative biases in the southeastern YRB. The explanations are that on the one hand, the upstream of the YRB is a mountainous region, where has only few rainfall stations and many of the rainfall stations located in the valley which may result in an underestimation of the rainfall. On the other hand, the resolution of topography used in the model of 15 km probably has an impact on the performance of rainfall. Previous studies found that the drag forces of the mesoscale (3-10 km) and microscale (<3 km) orography would prevent the moisture flux from being taken to the high-altitude complex terrain region (Wang et al., 2020). However, in our studies, the horizontal resolution of the inner domain is 15 km, which cannot take the mesoscale and microscale orography into account. Thus, the drag forces of the terrain are

https://doi.org/10.5194/hess-2020-441
Preprint. Discussion started: 14 September 2020


Hydrology and Earth System Sciences
Discussions

diminished, and more moisture is taken from the low-altitude region (i.e., the southeastern YRB) to the high-altitude region (i.e., the upstream of the YRB), which finally causes that the simulated rainfall tends to have positive biases in the high elevation area over the upstream of the YRB, and negative biases in the low elevation area over the southeastern YRB. We acknowledge that there are uncertainties from the bias of WRF modelling in the study, but the WRF model can still be used to investigate the impacts of LUCC and reforestation on summer rainfall. The only difference in the initial conditions used to force the WRF model for the four scenarios is the land cover. Thus, the changes in summer rainfall between different scenarios can be considered as the results of LUCC.

The changes in average summer rainfall show a large spatial heterogeneity between the 1990 and 2010 scenarios, while the extreme summer daily rainfall shows significant increases in most places of the midstream and downstream of the YRB. The main LUCC in the midstream and downstream of the YRB between the 1990 and 2010 scenarios was the rapid expansion of the urban area. Therefore, it can be inferred that urbanization may increase the intensity of extreme summer daily rainfall at a local scale. Similar results can be found in other studies. For example, Wang et al. (2015) found that extreme rainfall events had a strong positive spatial correlation with the urban extent. Zhang et al. (2018) also found that urbanization led to an amplification of the total rainfall along with a shift in the location of the maximum rainfall, and further increased the intensity and frequency of extreme flooding events.

The rainfall changes between the two hypothetical reforestation scenarios (20% and 50% scenarios) and the 2010 scenario reveal that transforming cropland to forest will increase summer rainfall. Comparing the simulation results from the whole YRB with results from grids where experienced LUCC, it can be seen that the impacts of LUCC on summer rainfall are mainly at the local scale. However, transforming different proportions of cropland to forest will have different impacts on local rainfall. With the transform proportion of cropland to forest increases from 20% to 50%, the impacts of the reforestation change from average rainfall increase to extreme rainfall increase. Besides, the SHF for the 50% scenario increases more than that for the 20% scenario, leading to a higher surface skin temperature, lower 2m relative humidity as well as an increased PBLH, which finally leads to more water vapor mixing in the atmosphere (Yu et al., 2017). All of the mentioned changes in thermodynamic variables provide conditions for more extreme rainfall increases (Zhang et al., 2019b).

Although a comprehensive assessment of the impacts of LUCC on summer rainfall amount and extremes was conducted in this study, some issues remained. For example, only one regional climate model (i.e., the WRF model) was used in this study, although it has been widely used in China (Huang et al., 2020;Azmat et al., 2020). Some previous studies indicated that results from one single RCM had a significant uncertainty since RCMs could perform differently in the same region (Davin et al., 2020;Zhang et al., 2017). In this case, it is worthwhile to look at the impacts of LUCC on summer rainfall and extremes based on the ensemble RCMs in future researches. Moreover, the random sampling method was used to produce the two hypothetical

https://doi.org/10.5194/hess-2020-441
Preprint. Discussion started: 14 September 2020


Hydrology and Earth System Sciences
Discussions

reforestation scenarios in this study. Thus, the grids where the cropland was changed to be forest tended to distributed evenly among the croplands in the YRB. But in fact, the reforestation process usually happened in specific areas that were relative to local policy. It was challenging to gather the related policies from multiple local governments over such a big basin. Despite this, this study could still provide a sight of what would happen to summer rainfall under reforestation.

6 Conclusions

In this study, analysis based on the WRF model simulations was used to research the impacts of LUCC and reforestation on summer rainfall amount and extremes in the YRB. Two observed scenarios (1990 and 2010 scenarios) were chosen to compare and investigate the changes in summer rainfall under the impacts of LUCC during the last decades. Besides, two hypothetical reforestation scenarios (20% and 50% scenarios) which were produced based on the 2010 scenario were used to test the sensitivity of summer rainfall to reforestation. The changes in summer rainfall between different scenarios were analyzed, and the potential mechanisms were discussed. The main conclusions are outlined below:

1. LUCC largely influenced summer rainfall amount and extremes during 1990-2010 in the YRB. The LUCC between the 1990 and 2010 scenarios decreases average summer rainfall, while increases extreme summer daily rainfall. The extreme summer daily rainfall increases up to 50 mm, which is mainly observed in the midstream and downstream.

2. Reforestation can affect heat flux, surface skin temperature, relative humidity and PBLH in the YRB, leading to more water vapor mixing in the atmosphere, which provides conditions for the increases of summer rainfall amount and extremes. And the effects of reforestation are more pronounced at the local scale where suffers reforestation than at the whole basin.

3. Although reforestation increases summer rainfall both in the amount and extremes, the differences exist in the scenarios with different reforestation proportions. More specifically, the average summer rainfall increases more for the scenario of 20% cropland changed to forest than that for the scenario of 50%, while the high-intensity short-duration rainfall increases more for the scenario of 50% cropland changed to forest than that for the scenario of 20%.

Acknowledgements

This work has been partially supported by the National Key Research and Development Program of China (Grant No. 2017YFA0603704), the National Natural Science Foundation of China (Grant No. 51811540407, 51779176), the Overseas Expertise Introduction Project for Discipline Innovation (111 Project) funded by Ministry of Education and State Administration of Foreign Experts Affairs P.R. China (Grant No. B18037), and the Center for Climate Dynamics (SKD) through the Bjerknes Centre for Climate Research (229200-FTI, CHEX). We thank Priscilla Mooney (NORCE) for providing

https://doi.org/10.5194/hess-2020-441
Preprint. Discussion started: 14 September 2020

her suggestions in the early analysis. The numerical calculations in this paper have been done on the supercomputing system in the Supercomputing Center of Wuhan University.

References

Azmat, M., Wahab, A., Huggel, C., Qamar, M. U., Hussain, E., Ahmad, S., and Waheed, A.: Climatic and hydrological projections to changing climate under CORDEX-South Asia experiments over the Karakoram-Hindukush-Himalayan water towers, Science of The Total Environment, 703, 135010, https://doi.org/10.1016/j.scitotenv.2019.135010, 2020.

Bennett, M. T., Mehta, A., and Xu, J.: Incomplete property rights, exposure to markets and the provision of environmental services in China, China Economic Review, 22, 485-498, https://doi.org/10.1016/j.chieco.2010.12.002, 2011.

Berrisford, P., Dee, D. P., Poli, P., Brugge, R., Mark, F., Manuel, F., Kållberg, P. W., Kobayashi, S., Uppala, S., and Adrian, S.: The ERA-Interim archive Version 2.0, ECMWF, Shinfield Park, Reading, 2011.

Chen, S.-H., and Sun, W.-Y.: A One-dimensional Time Dependent Cloud Model, Journal of the Meteorological Society of Japan. Ser. II, 80, 99-118, https://doi.org/10.2151/jmsj.80.99, 2002.

Cui, X., Liu, S., and Wei, X.: Impacts of forest changes on hydrology: a case study of large watersheds in the upper reaches of Minjiang River watershed in China, Hydrol. Earth Syst. Sci., 16, 4279-4290, https://doi.org/10.5194/hess-16-4279-2012, 2012.

Davin, E. L., Rechid, D., Breil, M., Cardoso, R. M., Coppola, E., Hoffmann, P., Jach, L. L., Katragkou, E., de Noblet-Ducoudré, N., Radtke, K., Raffa, M., Soares, P. M. M., Sofiadis, G., Strada, S., Strandberg, G., Tölle, M. H., Warrach-Sagi, K., and Wulfmeyer, V.: Biogeophysical impacts of forestation in Europe: first results from the LUCAS (Land Use and Climate Across Scales) regional climate model intercomparison, Earth System Dynamics, 11, 183-200, https://doi.org/10.5194/esd-11-183-2020, 2020.

Dudhia, J.: Numerical Study of Convection Observed during the Winter Monsoon Experiment Using a Mesoscale Two-Dimensional Model, Journal of the Atmospheric Sciences, 46, 3077-3107, https://doi.org/10.1175/1520-0469(1989)046<3077:NSOCOD>2.0.CO;2, 1988.

Fang, J., Tang, Y., and Son, Y.: Why are East Asian ecosystems important for carbon cycle research?, Sci China Life Sci, 53, 753-756, https://doi.org/10.1007/s11427-010-4032-2, 2010.

Feng, J.-M., Wang, Y.-L., Ma, Z.-G., and Liu, Y.-H.: Simulating the Regional Impacts of Urbanization and Anthropogenic Heat Release on Climate across China, Journal of Climate, 25, 7187-7203, https://doi.org/10.1175/JCLI-D-11-00333.1, 2012.

Feng, Y., Li, H., Tong, X., Chen, L., and Liu, Y.: Projection of land surface temperature considering the effects of future land change in the Taihu Lake Basin of China, Global and Planetary Change, 167, 24-34, https://doi.org/10.1016/j.gloplacha.2018.05.007, 2018.

Gao, F., de Colstoun, E. B., Ma, R., Weng, Q., Masek, J. G., Chen, J., Pan, Y., and Song, C.: Mapping impervious surface expansion using medium-resolution satellite image time series: a case study in the Yangtze River Delta, China, International Journal of Remote Sensing, 33, 7609-7628, https://doi.org/10.1080/01431161.2012.700424, 2012.

Gao, Q.-z., Wan, Y.-f., Xu, H.-m., Li, Y., Jiangcun, W.-z., and Borjigidai, A.: Alpine grassland degradation index and its response to recent climate variability in Northern Tibet, China, Quaternary International, 226, 143-150, https://doi.org/10.1016/j.quaint.2009.10.035, 2010.

Gao, Q., Li, Y., Wan, Y., Qin, X., Jiangcun, W., and Liu, Y.: Dynamics of alpine grassland NPP and its response to climate change in Northern Tibet, Climatic Change, 97, 515-528, https://doi.org/10.1007/s10584-009-9617-z, 2009.

Grell, G. A., and Dévényi, D.: A generalized approach to parameterizing convection combining ensemble and data assimilation techniques, Geophysical Research Letters, 29, 38-31-38-34, https://doi.org/10.1029/2002gl015311, 2002.

Hong, S.-Y., Dudhia, J., and Chen, S.-H.: A Revised Approach to Ice Microphysical Processes for the Bulk Parameterization of Clouds and Precipitation, Monthly Weather Review, 132, 103-120, https://doi.org/10.1175/1520-0493(2004)132<0103:ARATIM>2.0.CO;2, 2004.

Hong, S.-Y., Noh, Y., and Dudhia, J.: A New Vertical Diffusion Package with an Explicit Treatment of Entrainment Processes, Monthly Weather Review, 134, 2318-2341, https://doi.org/10.1175/MWR3199.1, 2006.

Hu, Y., Zhang, X.-Z., Mao, R., Gong, D.-Y., Liu, H.-b., and Yang, J.: Modeled responses of summer climate to realistic land use/cover changes from the 1980s to the 2000s over eastern China, Journal of Geophysical Research: Atmospheres, 120, 167-179, https://doi.org/10.1002/2014jd022288, 2015.

Huang, Y., Wang, Y., Xue, L., Wei, X., Zhang, L., and Li, H.: Comparison of three microphysics parameterization schemes in the WRF model for an extreme rainfall event in the coastal metropolitan City of Guangzhou, China, Atmospheric Research, 240, 104939, https://doi.org/10.1016/j.atmosres.2020.104939, 2020.

HURTT, G. C., FROLKING, S., FEARON, M. G., MOORE, B., SHEVLIAKOVA, E., MALYSHEV, S., PACALA, S. W., and HOUGHTON, R. A.: The underpinnings of land-use history: three centuries of global gridded land-use transitions, wood-harvest activity, and resulting secondary lands, Global Change Biology, 12, 1208-1229, https://doi.org/10.1111/j.1365-2486.2006.01150.x, 2006.

Hurtt, G. C., Chini, L. P., Frolking, S., Betts, R. A., Feddema, J., Fischer, G., Fisk, J. P., Hibbard, K., Houghton, R. A., Janetos, A., Jones, C. D., Kindermann, G., Kinoshita, T., Klein Goldewijk, K., Riahi, K., Shevliakova, E., Smith, S., Stehfest, E.,

Thomson, A., Thornton, P., van Vuuren, D. P., and Wang, Y. P.: Harmonization of land-use scenarios for the period 1500–2100: 600 years of global gridded annual land-use transitions, wood harvest, and resulting secondary lands, Climatic Change, 109, 117, https://doi.org/10.1007/s10584-011-0153-2, 2011.

Kain, J. S.: The Kain–Fritsch Convective Parameterization: An Update, Journal of Applied Meteorology, 43, 170-181, https://doi.org/10.1175/1520-0450(2004)043<0170:TKCPAU>2.0.CO;2, 2004.

Li, L., Gochis, D. J., Sobolowski, S., and Mesquita, M. D. S.: Evaluating the present annual water budget of a Himalayan headwater river basin using a high-resolution atmosphere-hydrology model, Journal of Geophysical Research: Atmospheres, 122, 4786-4807, https://doi.org/10.1002/2016jd026279, 2017.

Li, S., Xu, M., and Sun, B.: Long-term hydrological response to reforestation in a large watershed in southeastern China, Hydrological Processes, 28, 5573-5582, https://doi.org/10.1002/hyp.10018, 2014.

Li, W., Chen, J., and Zhang, Z.: Forest quality-based assessment of the Returning Farmland to Forest Program at the community level in SW China, Forest Ecology and Management, 461, 117938, https://doi.org/10.1016/j.foreco.2020.117938, 2020.

Liu, J., Liu, M., Deng, X., Zhuang, D., Zhang, Z., and Luo, D.: The land use and land cover change database and its relative studies in China, Journal of Geographical Sciences, 12, 275-282, https://doi.org/10.1007/BF02837545, 2002.

Liu, J., Liu, M., Zhuang, D., Zhang, Z., and Deng, X.: Study on spatial pattern of land-use change in China during 1995–2000, Science in China Series D: Earth Sciences, 46, 373-384, https://doi.org/10.1360/03yd9033, 2003.

Liu, J., Zhang, Z., Xu, X., Kuang, W., Zhou, W., Zhang, S., Li, R., Yan, C., Yu, D., Wu, S., and Jiang, N.: Spatial patterns and driving forces of land use change in China during the early 21st century, Journal of Geographical Sciences, 20, 483-494, https://doi.org/10.1007/s11442-010-0483-4, 2010.

Liu, J., Zhang, Q., and Hu, Y.: Regional differences of China's urban expansion from late 20th to early 21st century based on remote sensing information, Chinese Geographical Science, 22, 1-14, https://doi.org/10.1007/s11769-012-0510-8, 2012.

Liu, Y., Zhang, X., Xia, D., You, J., Rong, Y., and Bakir, M.: Impacts of Land-Use and Climate Changes on Hydrologic Processes in the Qingyi River Watershed, China, Journal of Hydrologic Engineering, 18, 1495-1512, https://doi.org/10.1061/(asce)he.1943-5584.0000485, 2013.

Mlawer, E. J., Taubman, S. J., Brown, P. D., Iacono, M. J., and Clough, S. A.: Radiative transfer for inhomogeneous atmospheres: RRTM, a validated correlated-k model for the longwave, Journal of Geophysical Research: Atmospheres, 102, 16663-16682, https://doi.org/10.1029/97JD00237, 1997.

Niu, G.-Y., Yang, Z.-L., Mitchell, K. E., Chen, F., Ek, M. B., Barlage, M., Kumar, A., Manning, K., Niyogi, D., Rosero, E., Tewari, M., and Xia, Y.: The community Noah land surface model with multiparameterization options (Noah-MP): 1. Model

description and evaluation with local-scale measurements, Journal of Geophysical Research: Atmospheres, 116, https://doi.org/10.1029/2010JD015139, 2011.

Pitman, A. J., de Noblet-Ducoudré, N., Avila, F. B., Alexander, L. V., Boisier, J. P., Brovkin, V., Delire, C., Cruz, F., Donat, M. G., Gayler, V., van den Hurk, B., Reick, C., and Voldoire, A.: Effects of land cover change on temperature and rainfall extremes in multi-model ensemble simulations, Earth System Dynamics, 3, 213-231, https://doi.org/10.5194/esd-3-213-2012, 2012.

Robbins, A. S. T., and Harrell, S.: Paradoxes and Challenges for China's Forests in the Reform Era, The China Quarterly, 218, 381-403, https://doi.org/10.1017/S0305741014000344, 2014.

Rogers, E., T. Black, B. Ferrier, Y. Lin, D. Parrish, and DiMego, G.: Changes to the NCEP Meso Eta Analysis and Forecast System: Increase in resolution, new cloud microphysics, modified precipitation assimilation, modified 3DVAR analysis., NWS Technical Procedures Bulletin, 2001.

Shem, W., and Shepherd, M.: On the impact of urbanization on summertime thunderstorms in Atlanta: Two numerical model case studies, Atmospheric Research, 92, 172-189, https://doi.org/10.1016/j.atmosres.2008.09.013, 2009.

Shen, S., Yue, P., and Fan, C.: Quantitative assessment of land use dynamic variation using remote sensing data and landscape pattern in the Yangtze River Delta, China, Sustainable Computing: Informatics and Systems, 23, 111-119, https://doi.org/10.1016/j.suscom.2019.07.006, 2019.

Skamarock, W. C., Klemp, J. B., Dudhia, J., Gill, , D. O., B., D., , and Duda, M. G.: A Description of the Advanced Research WRF Version 3 (No. NCAR/TN-475+STR), University Corporation for Atmospheric Research, https://doi.org/10.5065/D68S4MVH, 2008.

Sun, X., Li, C. a., Kuiper, K. F., Zhang, Z., Gao, J., and Wijbrans, J. R.: Human impact on erosion patterns and sediment transport in the Yangtze River, Global and Planetary Change, 143, 88-99, https://doi.org/10.1016/j.gloplacha.2016.06.004, 2016.

Taylor, K. E.: Summarizing multiple aspects of model performance in a single diagram, Journal of Geophysical Research: Atmospheres, 106, 7183-7192, https://doi.org/10.1029/2000JD900719, 2001.

Trac, C. J., Schmidt, A. H., Harrell, S., and Hinckley, T. M.: Is the Returning Farmland to Forest Program a Success? Three Case Studies from Sichuan, Environ Pract, 15, 350-366, https://doi.org/10.1017/S1466046613000355, 2013.

Wagner, S., Fersch, B., Yuan, F., Yu, Z., and Kunstmann, H.: Fully coupled atmospheric-hydrological modeling at regional and long-term scales: Development, application, and analysis of WRF-HMS, Water Resources Research, 52, 3187-3211, https://doi.org/10.1002/2015WR018185, 2016.

Wang, D., Jiang, P., Wang, G., and Wang, D.: Urban extent enhances extreme precipitation over the Pearl River Delta, China, Atmospheric Science Letters, 16, 310-317, https://doi.org/10.1002/asl2.559, 2015.

Wang, Y., Rhoads, B. L., Wang, D., Wu, J., and Zhang, X.: Impacts of large dams on the complexity of suspended sediment dynamics in the Yangtze River, Journal of Hydrology, 558, 184-195, https://doi.org/10.1016/j.jhydrol.2018.01.027, 2018.

Wang, Y., Yang, K., Zhou, X., Chen, D., Lu, H., Ouyang, L., Chen, Y., Lazhu, and Wang, B.: Synergy of orographic drag parameterization and high resolution greatly reduces biases of WRF-simulated precipitation in central Himalaya, Climate Dynamics, https://doi.org/10.1007/s00382-019-05080-w, 2020.

Wen, Q. H., Zhang, X., Xu, Y., and Wang, B.: Detecting human influence on extreme temperatures in China, Geophysical Research Letters, 40, 1171-1176, https://doi.org/10.1002/grl.50285, 2013.

Xue, H., Jin, Q., Yi, B., Mullendore, G. L., Zheng, X., and Jin, H.: Modulation of Soil Initial State on WRF Model Performance Over China, Journal of Geophysical Research: Atmospheres, 122, 11,278-211,300, https://doi.org/10.1002/2017JD027023, 2017.

Yang, Z.-L., Niu, G.-Y., Mitchell, K. E., Chen, F., Ek, M. B., Barlage, M., Longuevergne, L., Manning, K., Niyogi, D., Tewari, M., and Xia, Y.: The community Noah land surface model with multiparameterization options (Noah-MP): 2. Evaluation over global river basins, Journal of Geophysical Research: Atmospheres, 116, https://doi.org/10.1029/2010JD015140, 2011.

Yira, Y., Diekkrüger, B., Steup, G., and Bossa, A. Y.: Modeling land use change impacts on water resources in a tropical West African catchment (Dano, Burkina Faso), Journal of Hydrology, 537, 187-199, https://doi.org/10.1016/j.jhydrol.2016.03.052, 2016.

Yu, M., Miao, S., and Li, Q.: Synoptic analysis and urban signatures of a heavy rainfall on 7 August 2015 in Beijing, Journal of Geophysical Research: Atmospheres, 122, 65-78, https://doi.org/10.1002/2016JD025420, 2017.

Zhang, D., Liu, X., and Bai, P.: Assessment of hydrological drought and its recovery time for eight tributaries of the Yangtze River (China) based on downscaled GRACE data, Journal of Hydrology, 568, 592-603, https://doi.org/10.1016/j.jhydrol.2018.11.030, 2019a.

Zhang, H., Wu, C., Chen, W., and Huang, G.: Effect of urban expansion on summer rainfall in the Pearl River Delta, South China, Journal of Hydrology, 568, 747-757, https://doi.org/10.1016/j.jhydrol.2018.11.036, 2019b.

Zhang, J., Zhengjun, L., and Xiaoxia, S.: Changing landscape in the Three Gorges Reservoir Area of Yangtze River from 1977 to 2005: Land use/land cover, vegetation cover changes estimated using multi-source satellite data, International Journal of Applied Earth Observation and Geoinformation, 11, 403-412, https://doi.org/10.1016/j.jag.2009.07.004, 2009.

Zhang, W., Villarini, G., Vecchi, G. A., and Smith, J. A.: Urbanization exacerbated the rainfall and flooding caused by hurricane Harvey in Houston, Nature, 563, 384-388, https://doi.org/10.1038/s41586-018-0676-z, 2018.

https://doi.org/10.5194/hess-2020-441
Preprint. Discussion started: 14 September 2020

490 Zhang, X., Xiong, Z., Zhang, X., Shi, Y., Liu, J., Shao, Q., and Yan, X.: Simulation of the climatic effects of land use/land cover changes in eastern China using multi-model ensembles, Global and Planetary Change, 154, 1-9, https://doi.org/10.1016/j.gloplacha.2017.05.003, 2017.

Zhang, Y., Song, C., Zhang, K., Cheng, X., Band, L. E., and Zhang, Q.: Effects of land use/land cover and climate changes on terrestrial net primary productivity in the Yangtze River Basin, China, from 2001 to 2010, Journal of Geophysical Research:
495 Biogeosciences, 119, 1092-1109, https://doi.org/10.1002/2014JG002616, 2014.

Zinda, J. A., Trac, C. J., Zhai, D., and Harrell, S.: Dual-function forests in the returning farmland to forest program and the flexibility of environmental policy in China, Geoforum, 78, 119-132, https://doi.org/10.1016/j.geoforum.2016.03.012, 2017.

https://doi.org/10.5194/hess-2020-441
Preprint. Discussion started: 14 September 2020

Hydrology and Earth System Sciences
Discussions
Open Access
EGU

500 **Figures**

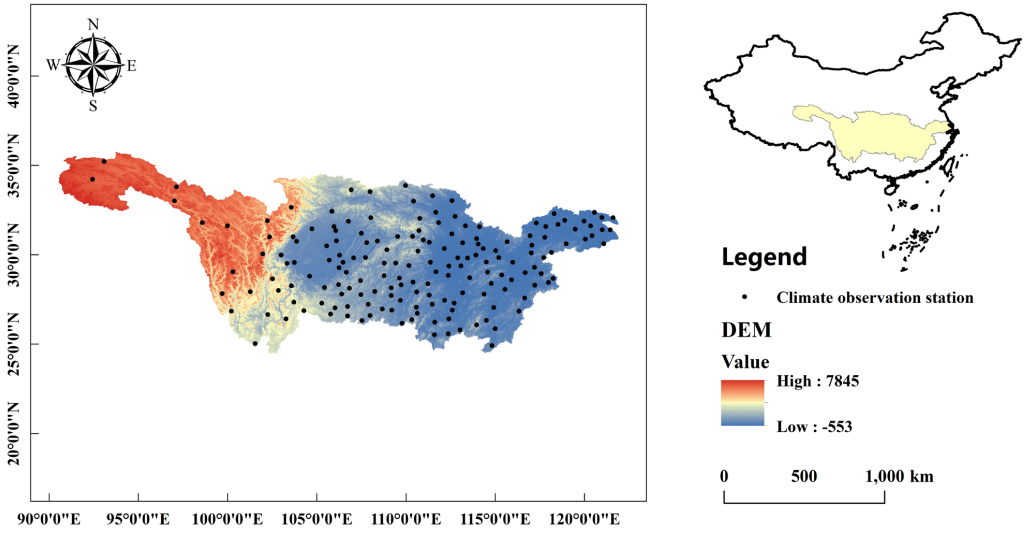

Figure 1. The location and topography of the Yangtze River Basin and the location of climate observation stations.

https://doi.org/10.5194/hess-2020-441
Preprint. Discussion started: 14 September 2020

Hydrology and Earth System Sciences
Discussions
Open Access
EGU

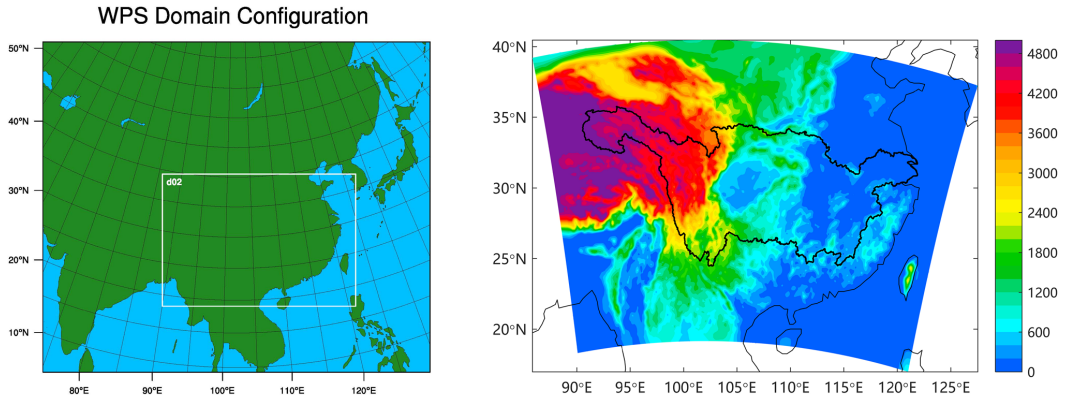

505 **Figure 2. The WRF model domain and the model topography (units: m).**

https://doi.org/10.5194/hess-2020-441
Preprint. Discussion started: 14 September 2020

Hydrology and Earth System Sciences
Discussions
Open Access
EGU

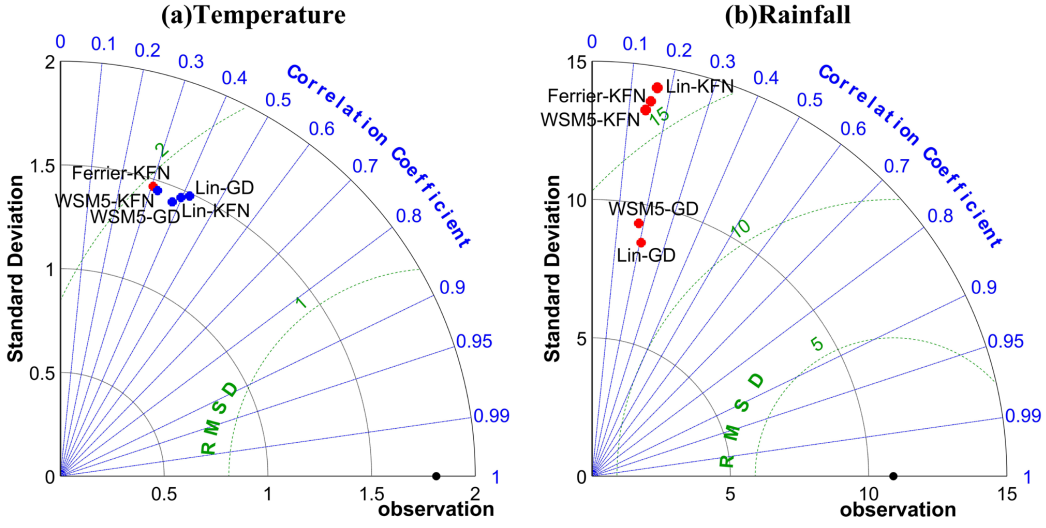

Figure 3. The Taylor diagrams of WRF parameterization schemes validation for (a) temperature and (b) rainfall.

https://doi.org/10.5194/hess-2020-441
Preprint. Discussion started: 14 September 2020

Hydrology and Earth System Sciences
Discussions
Open Access
EGU

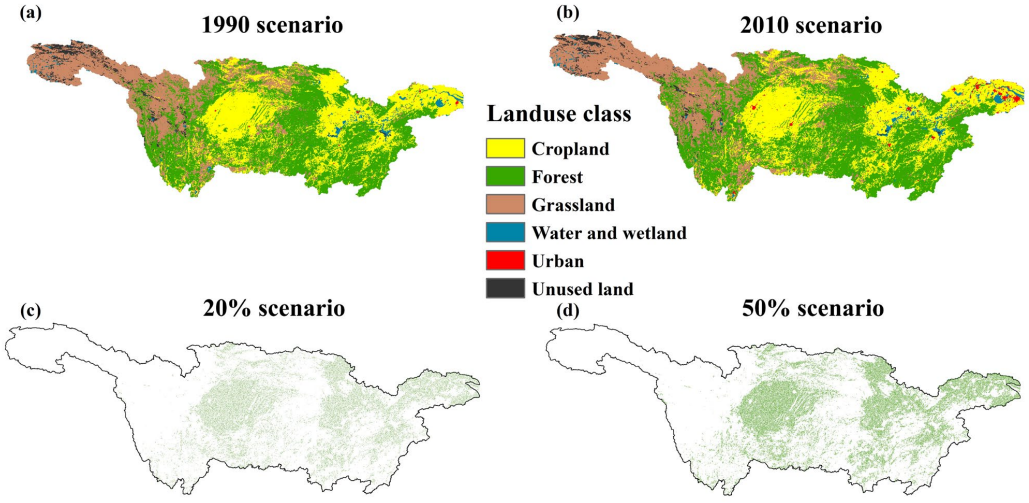

510

Figure 4. (a-b) Land use and cover under 1990 and 2010 scenarios; (c-d) Land use and cover changes between the 2010 scenario and two hypothesis scenarios (20% and 50% scenarios).

https://doi.org/10.5194/hess-2020-441
Preprint. Discussion started: 14 September 2020

Hydrology and Earth System Sciences
Discussions
Open Access
EGU

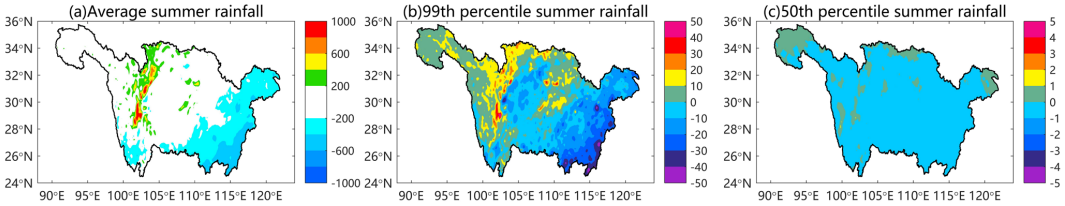

515 **Figure 5. The bias of (a) average summer rainfall (mm), (b) 99th percentile summer rainfall (mm/day) and (c) 50th percentile summer rainfall (mm/day) between the observed data and 2010 scenario.**

https://doi.org/10.5194/hess-2020-441
Preprint. Discussion started: 14 September 2020

Hydrology and Earth System Sciences
Discussions
Open Access
EGU

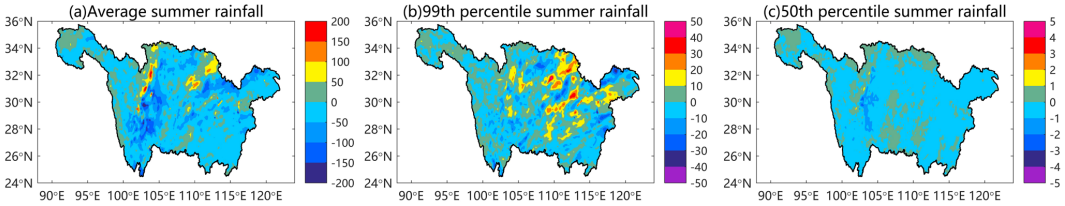

Figure 6. The changes in (a) average summer rainfall (mm), (b) 99th percentile summer rainfall (mm/day) and (c) 50th percentile summer rainfall (mm/day) between the 1990 scenario and 2010 scenario.

https://doi.org/10.5194/hess-2020-441
Preprint. Discussion started: 14 September 2020

Hydrology and Earth System Sciences
Discussions
Open Access
EGU

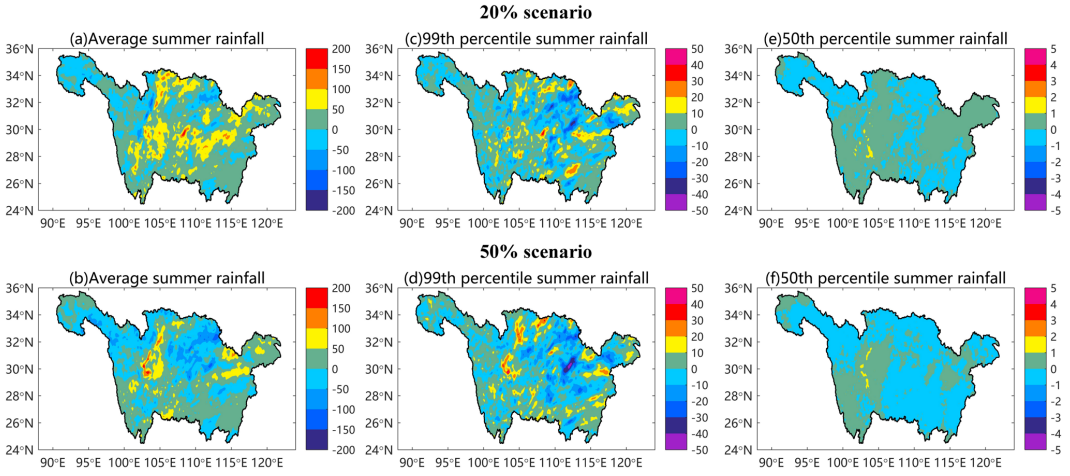

Figure 7. The changes in (a-b) average summer rainfall (mm), (c-d) 99th percentile summer rainfall (mm/day) and (e-f) 50th percentile summer rainfall (mm/day) between the 20% scenario and 2010 scenario, and between the 50% scenario and 2010 scenario.

525

https://doi.org/10.5194/hess-2020-441
Preprint. Discussion started: 14 September 2020

Hydrology and Earth System Sciences
Discussions
Open Access
EGU

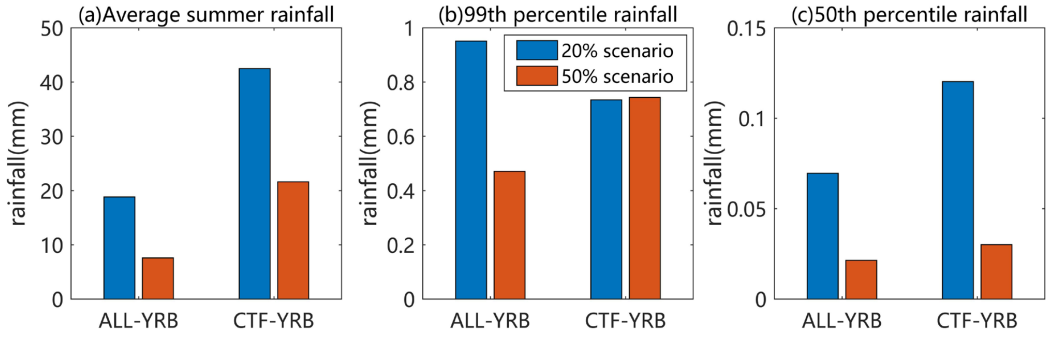

Figure 8. The changes in (a) average summer rainfall (mm), (b) 99th percentile summer rainfall (mm/day) and (c) 50th percentile summer rainfall between the 2010 scenario and two hypothesis scenarios (20% and 50% scenarios) in ALL-YRB and CTF-YRB area.

530

https://doi.org/10.5194/hess-2020-441
Preprint. Discussion started: 14 September 2020

Hydrology and Earth System Sciences
Discussions
Open Access
EGU

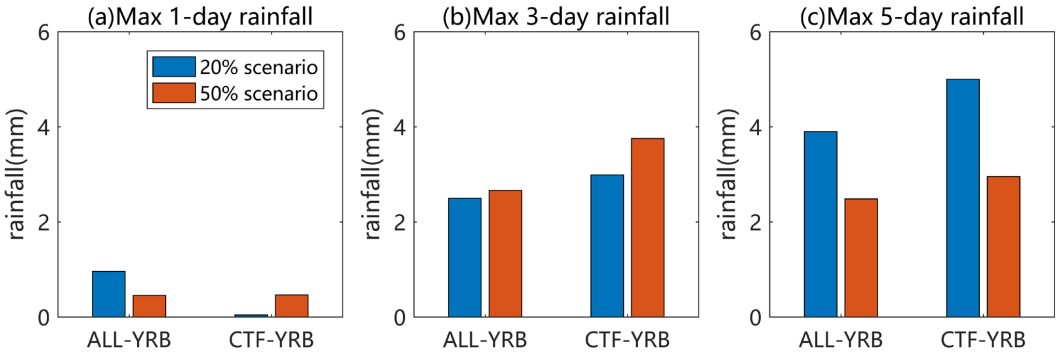

Figure 9. The changes in maximum 1-, 3-, 5-day rainfall between the 2010 scenario and two hypothesis scenarios (20% and 50% scenarios) in ALL-YRB and CTF-YRB area.

https://doi.org/10.5194/hess-2020-441
Preprint. Discussion started: 14 September 2020

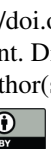

Hydrology and Earth System Sciences
Discussions
Open Access
EGU

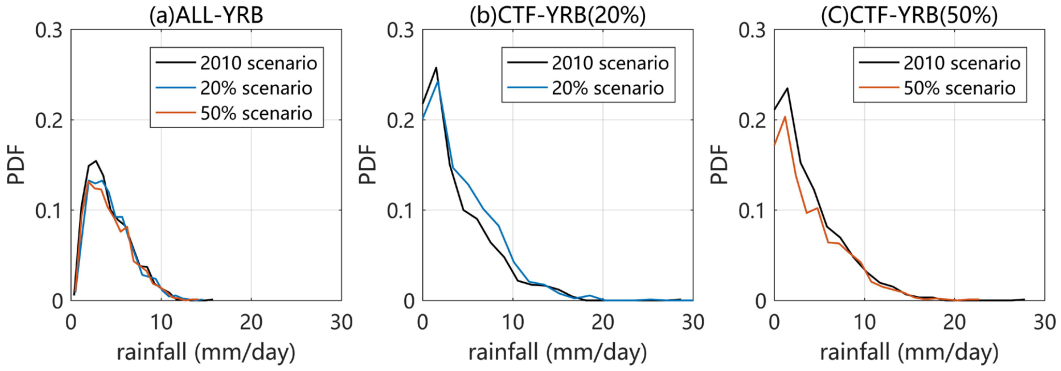

535

Figure 10. The probability distribution functions of summer rainfall in 2010, 20% and 50% scenarios in (a) ALL-YRB, (b) CTF-YRB (20%) and (c) CTF-YRB (50%).

https://doi.org/10.5194/hess-2020-441
Preprint. Discussion started: 14 September 2020

Hydrology and Earth System Sciences
Discussions
Open Access
EGU

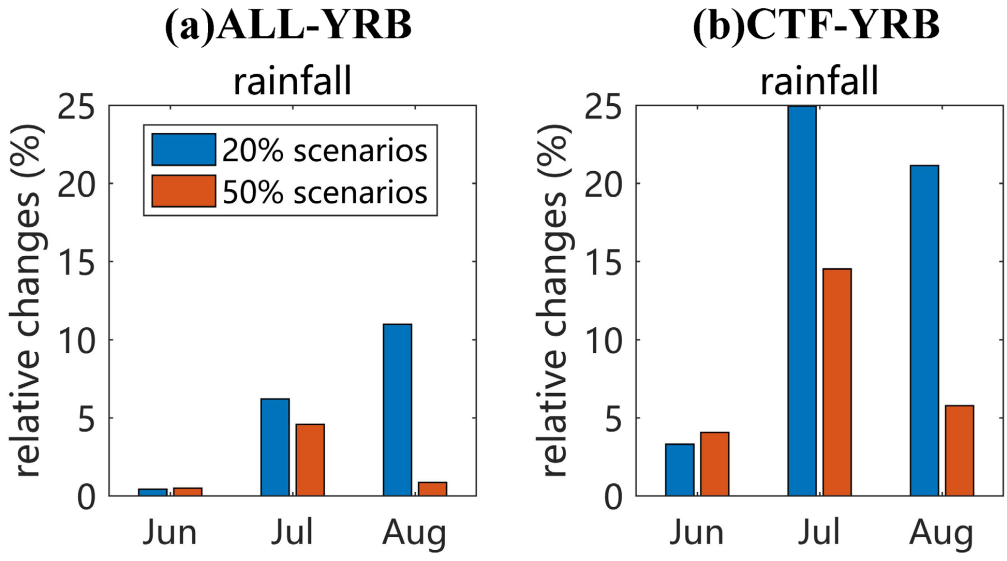

Figure 11. The changes in multi-year average summer monthly rainfall between the 2010 scenario and two hypothesis scenarios (20% and 50% scenarios) in (a) ALL-YRB and (b) CTF-YRB.

https://doi.org/10.5194/hess-2020-441
Preprint. Discussion started: 14 September 2020

Hydrology and Earth System Sciences
Discussions
Open Access
EGU

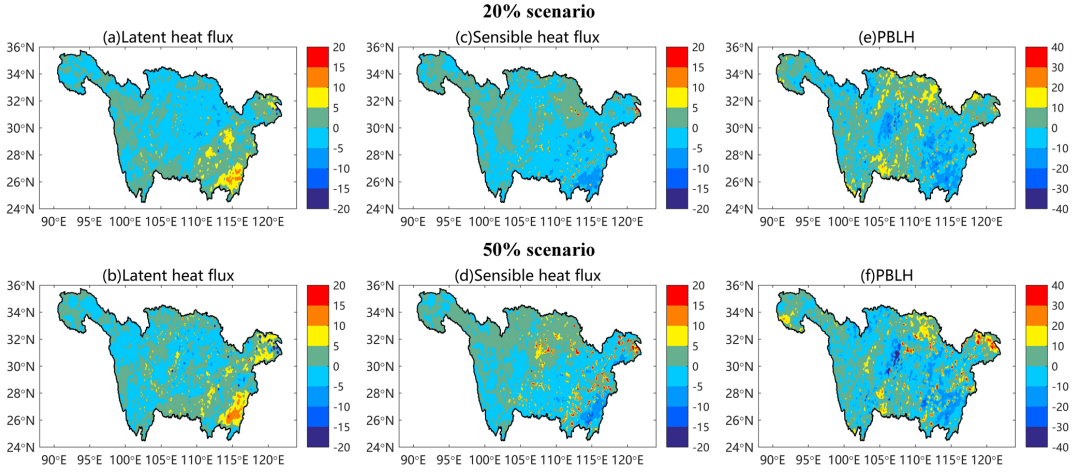

Figure 12. The changes in (a-b) latent heat flux (LHF, W/m^2), (c-d) sensible heat flux (SHF, W/m^2) and (e-f) PBL height (PBLH, m) between the 20% scenario and 2010 scenario, and between the 50% scenario and 2010 scenario.

https://doi.org/10.5194/hess-2020-441
Preprint. Discussion started: 14 September 2020

Hydrology and Earth System Sciences
Discussions
Open Access
EGU

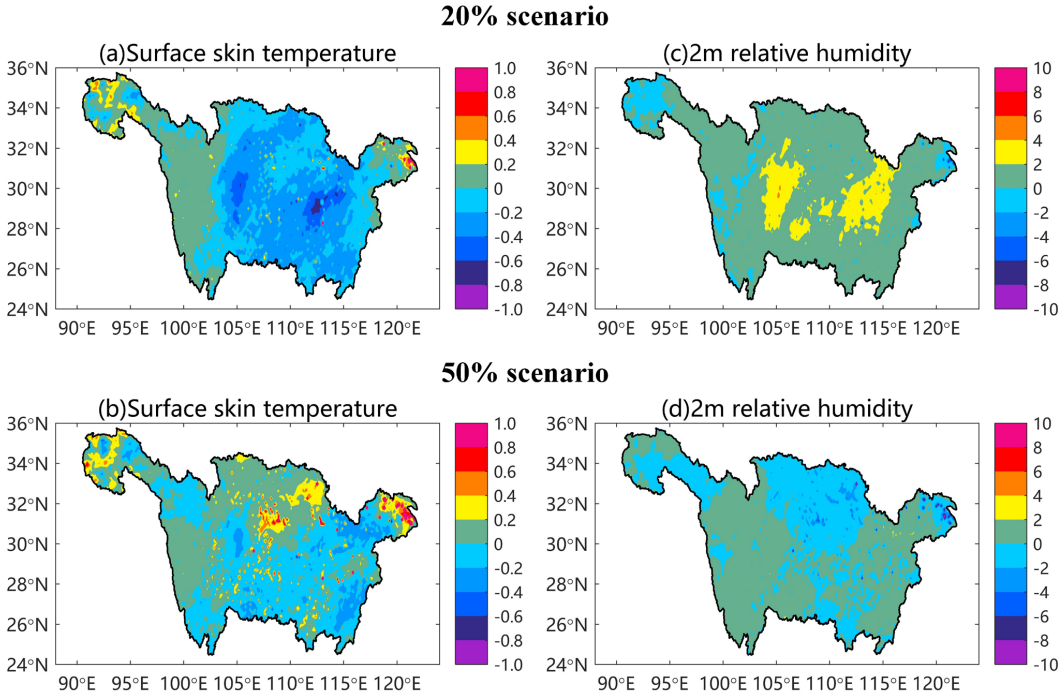

Figure 13. The changes in (a-b) surface skin temperature (℃) and (c-d) 2m relative humidity (%) between the 20% scenario and 2010 scenario, and between the 50% scenario and 2010 scenario.